IOP Conf. Series: Journal of Physics: Conf. Series **1308** (2019) 012006 doi:10.1088/1742-6596/1308/1/012006

State of the art measurements with TexAT

J Bishop[1,2], G V Rogachev[1,2], E Aboud[1,2], S Ahn[1], M Assunção[7], M Barbui[1], A Bosh[1,2], V Guimarães[5], J Hooker[1,2], C Hunt[1,2], D Jayatissa[1,2], E Koshchiy[1], S Lukyanov[6], R O'Dwyer[1,2], Y Penionzhkevich[6], E Pollacco[4], C Pruitt[3], B T Roeder[1], A Saastamoinen[1], L Sobotka[3], E Uberseder[1], S Upadhyayula[1,2], J Zamora[5]

[1] Cyclotron Institute, Texas A&M University, College Station, TX 77843, USA
[2] Department of Physics & Astronomy, Texas A&M University, College Station, TX 77843, USA
[3] Department of Chemistry, Washington University, St. Louis, USA
[4] IRFU, CEA Saclay, Gif-sur-Yvette, France
[5] Universidade de São Paulo, Brazil
[6] Flerov Laboratory of Nuclear Reactions, JINR, Dubna, Russia
[7] Universidade Federal de São Paulo, Brazil

E-mail: jackbishop@tamu.edu

Abstract. In the past several years, there has been a large interest of Time Projection Chambers (TPCs) for use in experimental nuclear physics. This has continued in tandem with the requirement for high efficiency detectors with low intensity radioactive ion beams. TexAT is a Active Target TPC (AT-TPC) built at Texas A&M University utilizing MICRO MEsh GASeous (MicroMegas) pads and GET electronics developed specifically for TPCs. This design combines good TPC pixelation with a surrounding shell of Si/CsI telescopes to make an extremely versatile detector capable of a wide range of different experimental techniques with only minor modifications to the electronics setup. Two recent experiments performed at the Cyclotron Institute, Texas A&M University, are detailed here demonstrating versatility beyond the usual Thick Target Inverse Kinematics (TTIK) or transfer reactions that these TPCs are more typically used for. The first, a measurement of the $^{12}\mathrm{N} \rightarrow {}^{12}\mathrm{C}^{\star} \rightarrow 3\alpha$ decay demonstrates the capabilities of TexAT as a low-energy detector operating at low pressure (20 Torr) to measure β-delayed particle decay. The second, a direct measurement of the $^{8}\mathrm{B}+{}^{40}\mathrm{Ar}$ fusion cross section shows the advantages of operating in active target mode where the target also functions as the detector gas.

1. Introduction

Time projection chambers (TPCs) offer many advantages over conventional charged-particle spectroscopy setups (necessitating their use with low intensity radioactive ion beams) and have become increasingly common e.g. [1–7]. TPCs operate by filling a chamber with a drift gas. As charged particles lose energy in the gas and liberate electrons along their path, these electrons are collected by a uniform electric field and produce a signal. Measuring the time of arrival and position of this signal, the 3D path of the particles can be reconstructed. These drifted electrons however typically only have an energy of $\sim$ eV therefore require significant amplification before they can be detected. MICRO MEsh GASeous (MicroMegas) detectors [8, 9] achieve this by a

IOP Conf. Series: Journal of Physics: Conf. Series **1308** (2019) 012006 doi:10.1088/1742-6596/1308/1/012006

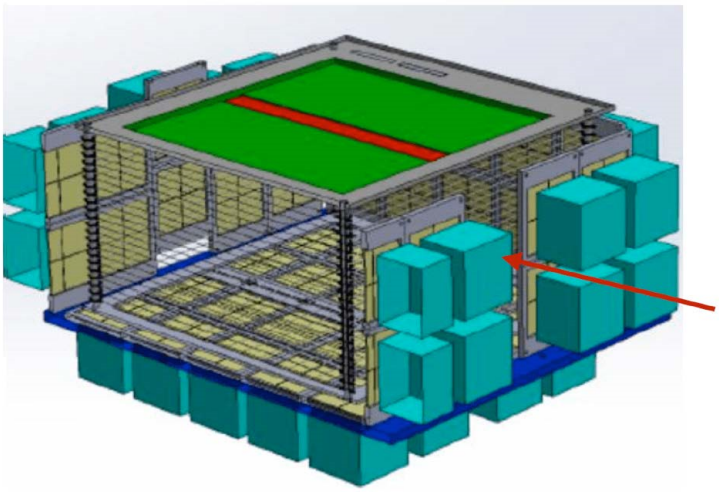

Figure 1. TexAT layout with the MicroMegas central pad (red) and side regions (green) surrounded by Si/CsI telescopes (cut-away view) following the future TexAT upgrade. The drift field is applied by the wires seen surrounding the active region.

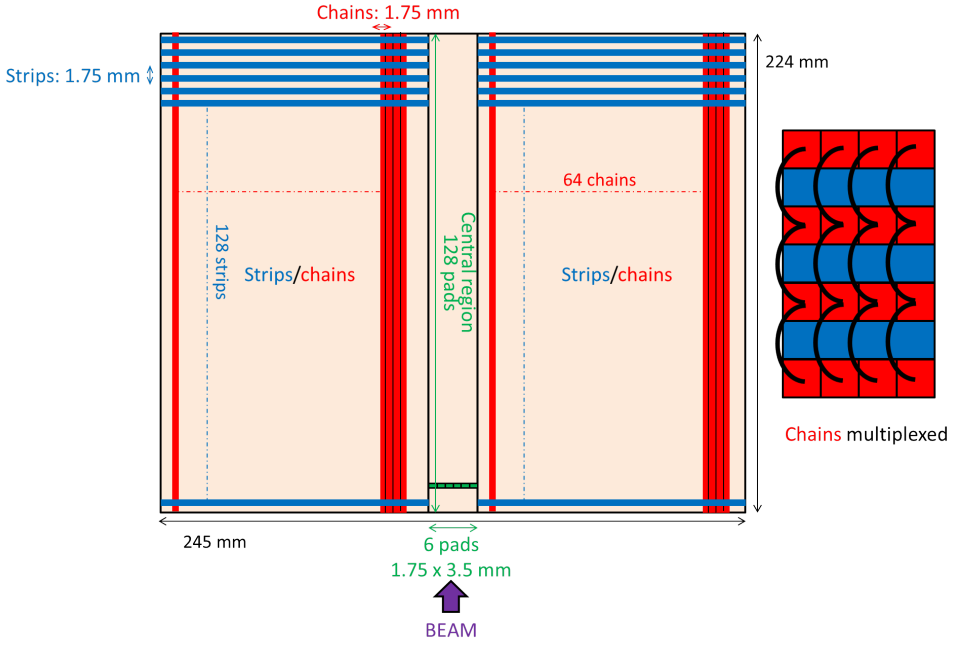

Figure 2. Layout of MicroMegas pads. There are two separate regions: the central region and the side regions with strips/chains. The central region contains 6 x 128 pads with a pitch of 1.75 mm in the beam direction and 3.5 mm in the perpendicular direction. These pads are read out individually. The side regions contains strips and chains which are multiplexed. The strips run perpendicular to the beam and run from the central region to the edge of the active area and constitute a continuous single strip. The chains are similarly multiplexed and run the length of this side region. These chains are spatially separated by the chains which run between them and are multiplexed as shown on the right by the black lines.

small amplification gap (128 μm) with a high voltage > 300 V. This large electric field generates a Townsend avalanche which can achieve a significant gain such that these drifted electrons can be detected. To maintain position sensitivity, the readout region is separated into pads with 1.75 mm pitch.

2. TexAT TPC

Fig. 1 shows TexAT, a TPC designed and built at the Cyclotron Institute, Texas A&M University [10–12]. The active region is 224 x 245 x 135 mm which is contained in an electric field provided by a field cage. At the top of the detector is a MicroMegas device which detects the drifted electrons created inside this active region. The pixelation provided by the MicroMegas pad is also shown in Fig. 2 where the increased pixelation in the centre region is apparent. This design also has a finer granularity in the beam direction. In the side regions, due to limitations in the number of readout channels, the pads require multiplexing for reading out. Horizontal (perpendicular to the beam direction) pads are read out together and are known as strips and the vertical pads (separated by the horizontal pads) are also multiplexed together and are known as chains. This multiplexing allows for a good granularity with a smaller number of readout channels required. Each readout channel is passed through into the GET electronics system [13] which has been specifically designed for TPCs. This system is shown in Fig. 3 where each channel can be seen to be fed into an AGET channel. This AGET chip digitises the signal at 25 MHz with 12 bit ADCs for 512 time buckets. Each channel also has an individual threshold which is fed into the MuTanT (MUltiplicity Trigger ANd Time) trigger unit.

3. Particle emission following β-decay

The flexibility of such a TPC as a probe of nuclear physics is vast. As a demonstration of this, an experiment was performed whereby states in ^{12}C above the α-decay threshold (7.37 MeV) were studied via the decay of ^{12}N. This β^+-decay has a half-life of 11.0 ms therefore must be investigated using the implantation technique rather than 'in-flight'. For this experiment, the main state of interest, the 0_2^+ resonance at 7.65 MeV known as the Hoyle state produces 3 α-particles which share 390 keV. This low energy therefore requires experimental care which is facilitated in this experiment by using a low pressure (20 Torr CO_2) fill gas in TexAT which gave the α-particles a long enough range that tracks can be measured. A decay-by-decay measurement

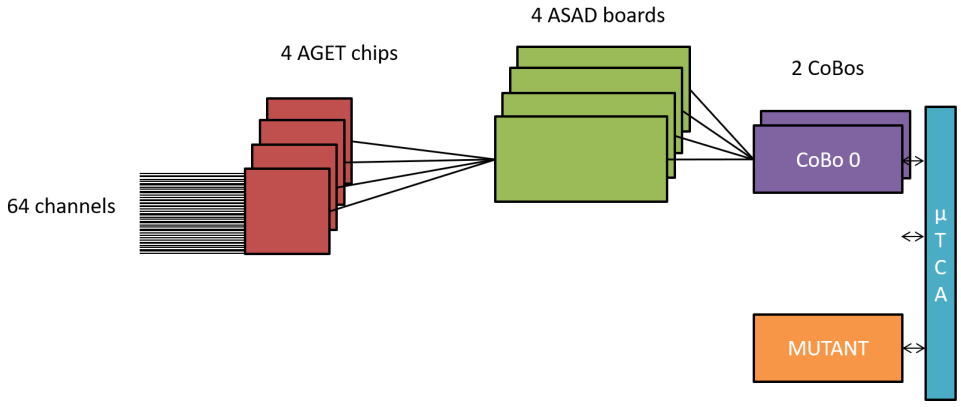

Figure 3. Electronics chain for the GET electronics system. Each CoBo (Concentration Board) supports 4 ASAD (ASIC ADC) boards which in turn support 4 AGET chips. These AGET chips can process 64 channels. The first CoBo is therefore sufficient to read out all 1024 channels of the MicroMegas allowing for 1024 channels from the second CoBo for Si/CsI detector channels.

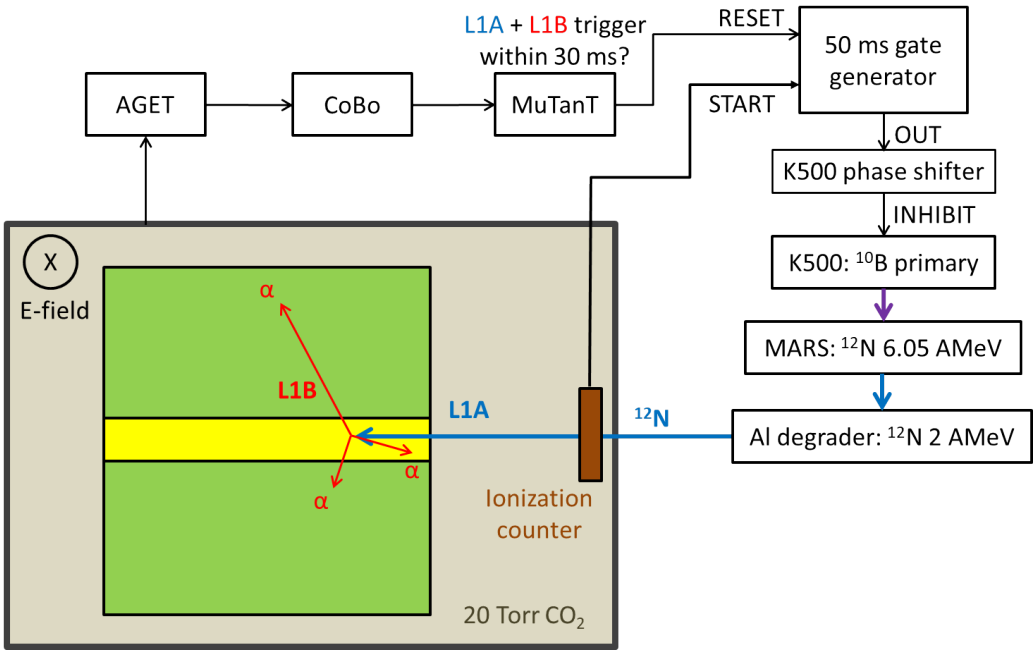

Figure 4. TexAT layout for the ^{12}N $\rightarrow 3\alpha$ experiment. The gate generator, triggered by the ion counter and reset by the successful measurement of a 3 α-particle decay feeds into the K500 cyclotron phase shifter. This allows for the beam to be stopped after an implantation has taken place.

can be achieved using the experimental setup shown in Fig. 4. This experiment was performed at the Cyclotron Institute, Texas A&M University, using the K500 cyclotron. The primary beam of ^{10}B then provided a ^{12}N secondary beam via the $(^3\mathrm{He}, n)$ reaction in the gas-cell on the MARS line. The secondary beam entered the detector at around 2 AMeV with a typical production intensity of 30 pps.

The measured data were split into two different frames using the 2p-mode in the GET electronics system [14] with two separate triggers. The first, the L1A trigger, corresponds to the track of the ^{12}N being implanted in the TPC and stopping. From this information, the decay position of the ^{12}N can be determined as well as verification via the energy deposited along its path that the track is a ^{12}N implant rather than a beam contaminant. The second trigger, the L1B, corresponds to the 3 α-particle decay of states in ^{12}C following the β^+-decay of ^{12}N . For both the L1A and the L1B, a pad multiplicity of > 1 is required for a duration of 10 timebuckets (a total of 400 ns) in the MicroMegas to generate this trigger. The TPC allows for 3D tracks of the three α-particles to be reconstructed. By measuring the total energy deposited, the excitation energy can be calculated by $E_x = E_{\mathrm{measured}} + Q$. Additionally, selecting tracks where the range of the α-particles correspond to that expected from the decay of the Hoyle state (with the maximum α-particle energy being 190 keV), a clean selection on Hoyle decays can be achieved, as seen in Fig. 5 for a subset of the data. The counts excluded from this cut arise from higher lying states in ^{12}C which have higher energy α-particles which escape the MicroMegas and therefore do not deposit their full energy, instead creating a smooth distribution at higher energies.

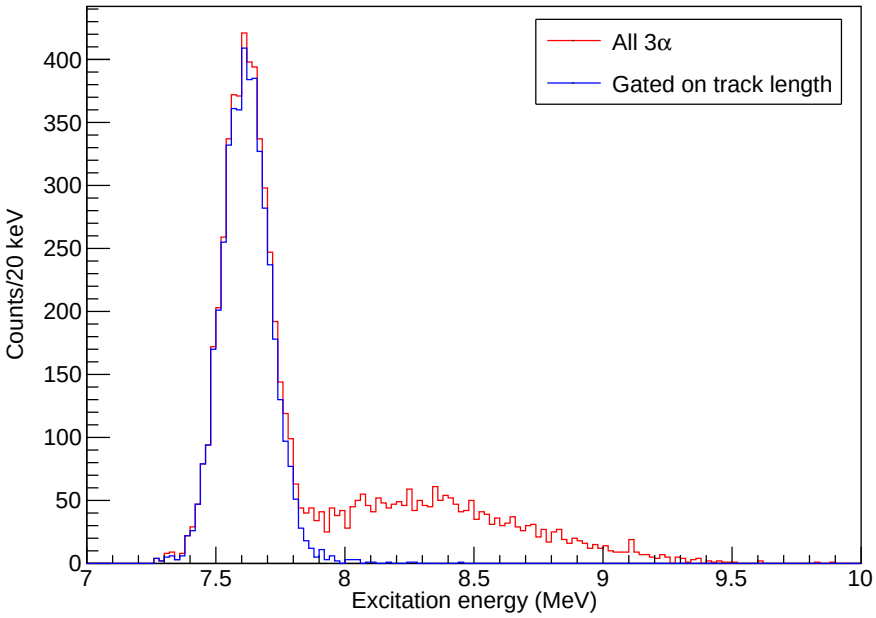

Figure 5. Excitation function for 3 α-particle events following the decay of ^{12}N calculated from the total energy deposited in the TPC. The gate corresponds to selecting events where the longest α-particle track is commensurate with a 190 keV energy corresponding to the decay of the Hoyle state into ^{8}Be(g.s) + α.

4. Direct fusion measurement

Traditional measurements of fusion cross sections across a wide energy range require measuring a particular exit channel and using models to then convert to the total cross section. By utilising a TPC as an active target, this fusion cross section can be measured directly across a wide range of energies. This technique relies on a measurement of the energy deposition as the impinging beam slows down in the target gas and then undergoes fusion. As the compound nucleus then splits into two (or more) fragments, the energy is then shared so as to conserve momentum. This spreading out of energy (in addition to the large increase in A and Z of the heavy recoil) means the energy deposition per unit length vastly increases. The identification of this vertex position then can be used to identify the centre of mass energy of the collision given the initial beam energy and the distance travelled in the gas. An accumulation of thousands of such events then gives a cross section measurement after correcting for the effective target thickness.

Of particular interest is the measurement of the ^{8}B + ^{40}Ar fusion cross section. As ^{8}B is a lightly-bound nucleus, believed to be a one-proton halo [15], the effect of this structure has an underlying effect on the fusion cross section as well as the ^{7}Be$(p,\gamma)^{8}$B reaction in main sequence stars. It has been found that the total fusion cross section is systematically lower for these weakly bound systems [16]. Careful investigation is therefore required to understand the role of coupling to the continuum.

The measurement of the ^{8}B + ^{40}Ar fusion cross section was therefore measured using TexAT with P_5 fill gas (95% Ar + 5% CH_4) at 150 Torr. To reduce the read-out rate of the TPC to avoid considerable dead-time for a high intensity beam such as ^{8}B, the MicroMegas were used in tandem with an ion counter placed at the entrance of the chamber. The signal of the ^{8}B passing through the ion counter provided a trigger for the acquisition while the last eighth of the

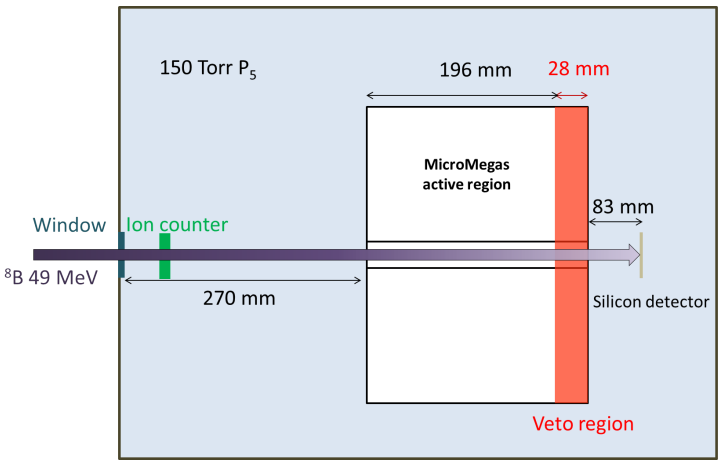

Figure 6. Experimental setup for direct fusion measurement. The TexAT chamber was filled with 150 Torr P5 gas. A 49 MeV ^{8}B enters the chamber and provides a trigger via an ion counter. The beam has sufficient energy to stop in a silicon detector placed at zero degrees. Upon traversing the last eight of the MicroMegas, a signal from this region is used to veto the ion counter signal. Therefore, only events which stop before the veto region are accepted. This removes non-interacting beam events and leaves breakup, fusion and elastic scattering events which are written to disk.

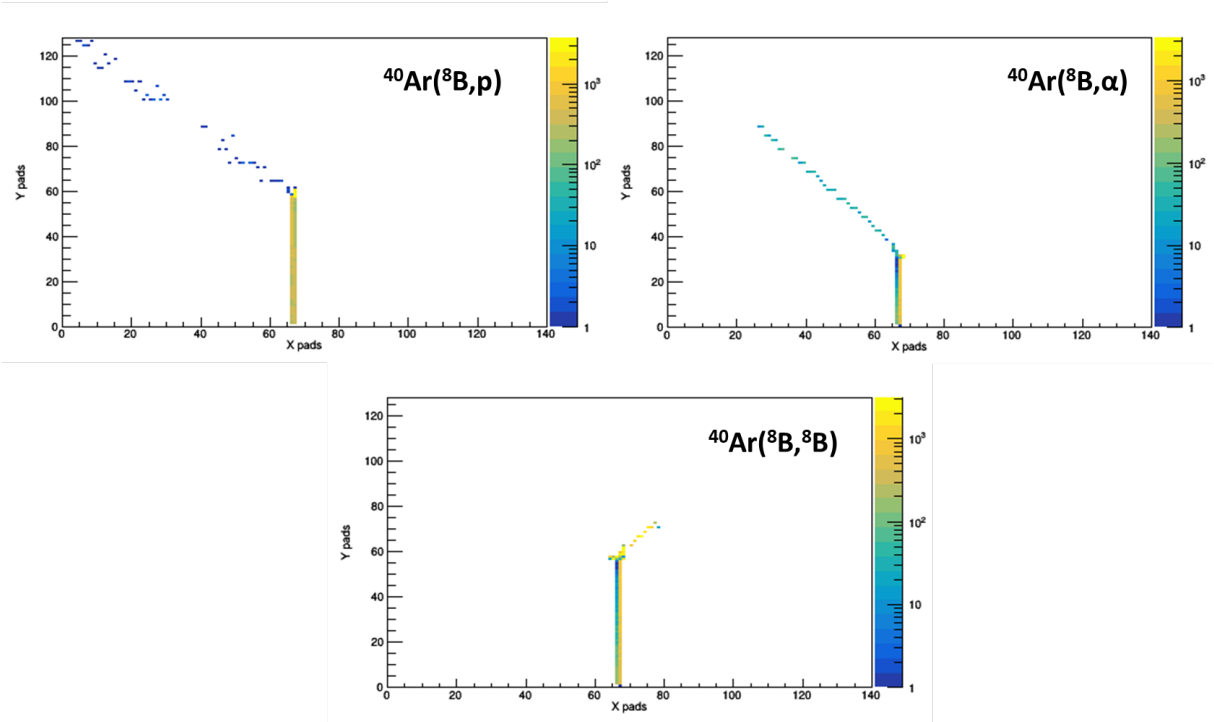

Figure 7. Top: GEANT4 simulated MicroMegas tracks. Top left: $^{40}\mathrm{Ar}(^{8}\mathrm{B}, p)$. Top right: $^{40}\mathrm{Ar}(^{8}\mathrm{B}, \alpha)$. Bottom: $^{40}\mathrm{Ar}(^{8}\mathrm{B}, ^{8}\mathrm{B})$. In all these exit channels, the heavy recoil has a very short range and therefore deposits all of its energy at the interaction vertex. In the proton evaporation channel, the proton has enough energy to enter the veto region but is sufficiently high energy that the energy loss along the track is below the detection threshold therefore does not veto the event.

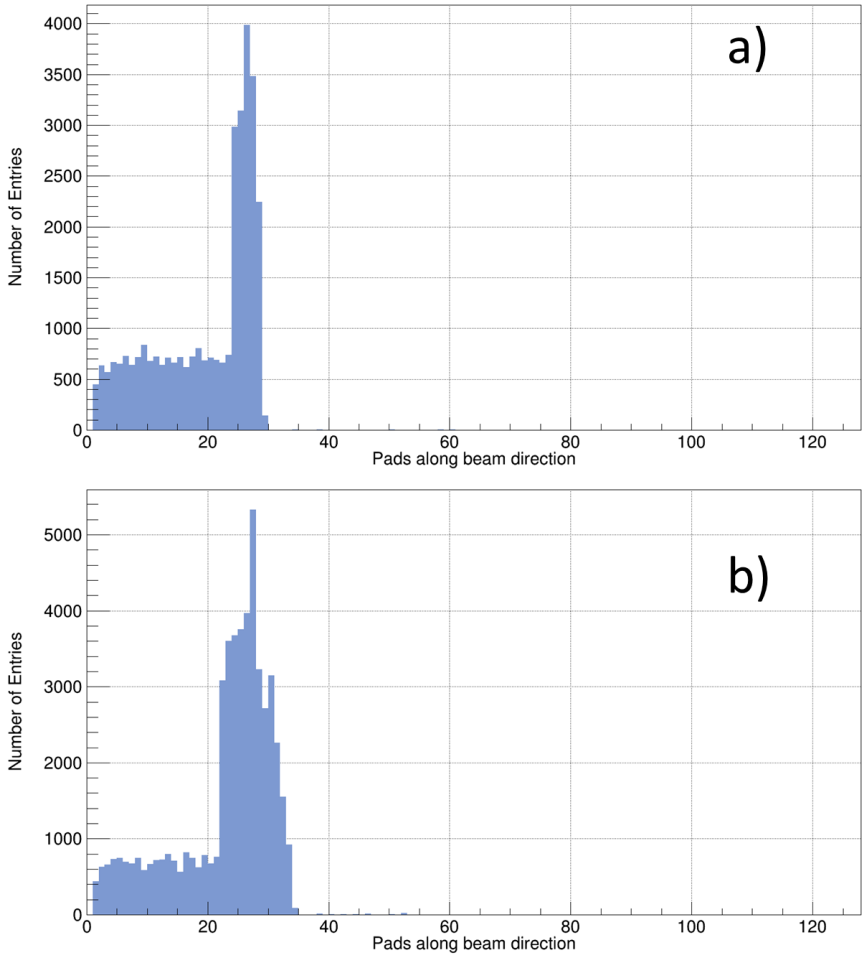

Figure 8. a) Energy loss as a function of distance traveled along the MicroMegas for the ^{40}Ar(^{8}B, ^{4}He)^{44}Sc reaction. b) Same plot but for ^{12}C(^{8}B, ^{4}He)^{16}F corresponding to interactions with the 5% methane in the P5 gas. While the peak signal is similar for the two processes, the width of the peak for the Ar interaction is narrower by virtue of the reduced range of the recoiling ^{44}Sc versus the ^{16}F.

MicroMegas allowed for a veto signal to be given to the readout. If the ^{8}B does not undergo an interaction with the gas (break-up/fusion/elastic scattering) then the beam has sufficient energy to traverse the MicroMegas and hit a silicon detector at zero degrees. This will therefore provide both a trigger (from the ion counter) and a veto (from the MicroMegas). If an interaction were to take place, then the outgoing particles will have lost sufficient energy that they will stop in the gas before reaching the veto region and the event is taken. Therefore, in this configuration, only events where the beam loses sufficient energy to not reach the end region of the detector are read out. This layout is summarized in Fig. 6.

This reaction was modelled in GEANT4 and can be seen in Fig. 7 for the proton - ^{40}Ar(^{8}B, p), α-particle - ^{40}Ar(^{8}B, α) and compound-elastic channel - ^{40}Ar(^{8}B, ^{8}B). The proton channel is such that the proton can easily enter the veto region however due to the energy deposition per unit length (which is $\sim$ 40 times lower than the incoming beam), the proton track is below the detection threshold so does not veto the event.

Additionally, it is important to model the interaction of the beam with carbon in the methane which constitutes a background to the measurement. A separate run was performed with pure methane in order to allow for background subtraction. However on an event-by-event basis, the separation of interactions with argon or carbon was investigated. The energy loss along the beam direction is shown in Fig. 8 for these two scenarios with an interaction at the same position along the MicroMegas in the α-evaporation channel. The energy loss profile has a very similar peak size for the two interactions however the interaction with the argon has a much sharper peak due to the smaller range of the ^{44}Sc heavy recoil versus the recoiling ^{16}F for carbon fusion. By virtue of the mass disparity between the two, the fusion event with carbon also provides the heavy recoil with a larger total energy in comparison with the argon. As an example, for a 20 MeV ^{8}B undergoing fusion and exiting via the proton channel at $\theta_p = 55^\circ$ in the lab, the argon fusion's heavy recoil (^{47}Ti) has an energy of 2.3 MeV in comparison with 6.2 MeV for the carbon fusion's heavy recoil (^{19}Ne). This can clearly be seen by the larger integral over the peak of Fig. 8 for the carbon interaction corresponding to a larger overall energy deposition.

5. Conclusion

As evidenced by these two studies, TexAT is able to facilitate a wide range of different techniques in addition to elastic scattering experiments most typically performed using this type of equipment. A combination of good central granularity of the MicroMegas coupled with sufficient gains allows for a good study of low energy-charged particles which may be used for a wide range of β-delayed charged particle experiments using the same 2p-mode implantation technique. Additionally, the GET electronics design allows for a versatile range of trigger conditions. This allows for high levels of trigger selection, without which, the TPC would become saturated with dead time. TexAT continues to be upgraded with a recently installed GEM layer [17] providing additional gain allowing for light particle tracks to be measured. Finally, the implementation of the higher coverage Si/CsI telescopes surrounding the MicroMegas region is currently under way, further increasing this device's capabilities.

References

[1] Hong B *et al* 2014 *Eur. Phys. J. A* ***50*** *49*
[2] Vorobyov A A *et al* 1988 *Nucl. Instrum. Methods Phys. Res. A* **270**, 419–30
[3] Roger T *et al* 2018 *Nucl. Instrum. Methods Phys. Res. A* **895**, 126–34
[4] Demonchy C E *et al* 2007 *Nucl. Instrum. Methods. Phys. Res. A* **583** 341–9
[5] Mizoi Y *et al* 1999 *Nucl. Instrum. Methods. Phys. Res. A* **431** 112–22
[6] Suzuki D *et al* 2012 *Nucl. Instrum. Methods. Phys. Res. A* **691** 39-54
[7] Beceiro-Novo S *et al* 2015 *Prog. Part. Nucl. Phys.* **84** 124–585
[8] Giomataris Y, *et al* 1996 *Nucl. Instrum. Methods Phys. Res. A* **376** 29-35
[9] Suzuki D, *et al* 2011 *Nucl. Instrum. Methods Phys. Res. A* **660** 64–8
[10] Koshchiy E *et al* Status of Texas Active Target (TexAT) detector
[11] Uberseder E *et al* Texas active target (TexAT) detector - part 2: Monte Carlo simulations
[12] Uberseder E *et al* Texas active target (TexAT) detector - part 3: Acquisition and analysis infrastructure
[13] Pollacco E C *et al* 2018 *Nucl. Instrum. Methods Phys. Res. A* **887**, 81-93
[14] Giovinazzo J *et al* 2007 *Phys. Rev. Lett.* **99**, 102501
[15] Minamisono T *et al* 1992 *Phys. Rev. Lett.* **69**, 2058
[16] Lei J and Moro A M 2019 *Phys. Rev. Lett.* **122**, 042503
[17] Kaminski J *et al* 2004 *Nucl. Instrum. Methods Phys. Res. A* **535** 201–5